# A boundary observable compared in U(1) and SU(2) lattice gauge theory: one loop, a strong-coupling sign and Monte Carlo

Kiichi Shiori Rin

2026-10-29 (revised 2026-11-14; text revised 2026-11-15)

wvbks0 [at] gmail.com · https://computoergosum.com/en/index.html

AI use is disclosed in §9; what is not claimed is in §7.

**Abstract**

In the Schrödinger functional of four-dimensional lattice gauge theory we separate the boundary angle into a lower angle $\alpha$ and an upper angle $\gamma$. In this setting we compare two quantities normalised to equal the bare coupling $\beta$ at tree level: the usual Schrödinger-functional coupling $\beta_R = 4/\bar{g}^2$, a first derivative at the symmetric point, and $D_R$, a finite-difference version of the mixed derivative $\partial^2 \ln Z/\partial\alpha\,\partial\gamma$. The mixed derivative contains no contact term and drops every free energy that depends on one boundary only. We study $h := \beta_R - D_R$ in three regimes. At one loop (SU(2), Wilson action, $L/a = 4$ to 24, computed directly on the lattice) the coefficient of $\ln(L/a)$ in $D_R$ equals the predicted $-8b_0$ to within 1% (fits with $L/a \geq 8$), as does that of $\beta_R$. In the same computation the constants differ by 0.21, so that $h \to -0.21$, and the difference between $\beta_R$ and the mixed derivative $M_R$ at the symmetric point comes entirely from the charged fluctuations. This difference is zero in the neutral sector, which suggests (without a separate computation) that it vanishes for U(1). At strong coupling, for fixed $L/a \geq 4$ and under an assumption (H) that the remainder beyond the strip and cylinder terms is $O(u^{3L+1})$, $h < 0$ with leading term $-(8/s)u^{3L}$, $s = \sin(\pi/(2L^2))$. This assumption contains both the convergence of the polymer expansion and the completeness of our hand count of the leading terms, and the sign follows from it almost at once. The arithmetic and inequality steps of this argument are written in Lean 4 and pass its check. A Monte Carlo study on one laptop (SU(2): 36 points, $L/a = 3$ to 8; U(1): 21 points) gives the shape of $h$ as a function of $\bar{g}^2$: $h$ is compatible with zero near $\bar{g}^2 \approx 4.8$ and clearly positive from $\bar{g}^2 \approx 5.5$, has a maximum 0.14 to 0.18 for $\bar{g}^2 \approx 5$ to 10, returns to zero for $\bar{g}^2 \approx 60$ to 120 and lies between $-0.03$ and 0 beyond. In these data, for $L/a \geq 4$ and $\bar{g}^2 \approx 35$ to 140, the lattice sizes agree point by point within about $2\sigma$. In U(1), $h$ is compatible with zero deep in the Coulomb and in the confined phase, and has a peak at the transition whose height does not decrease at $L/a = 8$. The size of $h$ thus distinguishes the two theories in these data only away from the U(1) transition, and the two are not compared at the same $\bar{g}^2$. The status of the paper is computer-assisted, with Lean for the arithmetic steps, and conditional on the assumptions listed in §6.

## 1 Introduction

The question behind this note is the mass-gap problem for four-dimensional Yang–Mills theory (Clay Millennium Problem, statement by Jaffe and Witten [1]). Nothing here addresses that problem directly. We look for a single, well-defined lattice observable whose shape as a function of the renormalised coupling separates the non-abelian theory from compact U(1), which has a massless Coulomb phase. The data below separate the two only away from the U(1) transition and not at the same renormalised coupling (§5). The Schrödinger-functional

(SF) coupling of Lüscher, Narayanan, Weisz and Wolff [2] and of Lüscher, Sommer, Weisz and Wolff [3] is such an observable in the weak-coupling region, but it is a first derivative with respect to a boundary angle that moves both boundaries at once. In the strong-coupling region the SF coupling therefore picks up free-energy contributions that live at one boundary only (in the strong-coupling expansion, strips of plaquettes winding around one boundary). These contributions are not related to the propagation of flux between the two boundaries.

We replace the first derivative by the mixed second derivative with respect to the two boundary angles. The idea is elementary: if $\Gamma = -\ln Z$ is written as $f(\alpha) + f(\gamma) + g(\alpha, \gamma)$, the mixed derivative kills $f$ exactly and measures only $g$. This note records what we found in three regimes for the difference $h = \beta_R - D_R$ between the usual SF coupling and the mixed-derivative quantity:

1. a one-loop computation on the lattice (§3);
2. the sign of $h$ in the strong-coupling expansion, at fixed $L/a \geq 4$, with the arithmetic steps written in Lean 4 (§4);
3. a Monte Carlo study of $h$ as a function of $\bar{g}^2 = 4/\beta_R$ for SU(2), and of $h$ for U(1) as a control (§5).

The SF coupling itself, its one-loop coefficient and the renormalisability argument are from [2, 3]. We reproduce the one-loop coefficient table of [2] as a check of our code. The use of the mixed derivative as a separate observable, and the numbers below, are what this note adds. We do not know whether the same observable has been studied before. Numbers quoted without a citation are taken from the authors' working records (programs, outputs and reports), which are not published.

**Status of the results.** The results are computer-assisted (floating-point one-loop and Monte Carlo, not interval arithmetic), with the arithmetic and inequality steps of the strong-coupling sign in Lean 4. The strong-coupling statement is conditional on the convergence of the polymer expansion and on the coefficients of the leading terms, which are derived by hand. No statement of this note is an unconditional theorem about the continuum theory.

# 2 Setting and definitions

## 2.1 The Schrödinger functional with two boundary angles

We use the SF of [2, 3] for gauge group SU(2). The lattice is $L^3 \times L$ (lattice units, $a = 1$), periodic in the three spatial directions, with Dirichlet boundary conditions at $x^0 = 0$ and $x^0 = L$. The action is the Wilson action $S = \beta \sum_p w(p)\,(1 - \frac{1}{2}\,\mathrm{tr}\,U_p)$ with weight $\frac{1}{2}$ on the spatial plaquettes of the two boundaries and $c_t = 1$ (no $O(a)$ boundary improvement), and $\beta = 4/g_0^2$. The spatial links at $x^0 = 0$ are $\exp\{(\alpha/L)\,\tau\}$ and those at $x^0 = L$ are $\exp\{(\gamma/L)\,\tau\}$, with $\tau$ the fixed Cartan generator. The holonomies around a spatial cycle are therefore $W_0 = e^{\alpha\tau}$ and $W_L = e^{\gamma\tau}$. The usual SF is $\alpha = \eta$, $\gamma = \pi - \eta$ [3, (2.5),(2.6)]. The induced classical field is a constant colour-electric field depending on $\gamma - \alpha$ only, and the classical action [3, (2.11)], rewritten for two angles, is

$$S_{\mathrm{cl}} = 3\beta L^4 (1 - \cos((\gamma - \alpha)/L^2)). \tag{1}$$

For U(1) we use the same geometry and the same normalising formulas (so that at tree level all quantities below equal $\beta$), with $\bar{g}^2 := 1/\beta_R$.

Let $\Gamma(\alpha, \gamma) = -\ln Z(\alpha, \gamma)$.

**Definition 2.1** (the two observables)**.** (i) The SF coupling at $\eta = \pi/4$: with $\alpha = \eta$, $\gamma = \pi - \eta$, so that $\partial_\eta = \partial_\alpha - \partial_\gamma$,

$$\beta_R := \frac{\langle \partial_\alpha S - \partial_\gamma S \rangle}{-6L^2 \sin(\pi/(2L^2))} \qquad (\alpha = \pi/4,\ \gamma = 3\pi/4),$$

equal to $\beta$ at tree level by (1); $\bar{g}^2 := 4/\beta_R$ for SU(2).

(ii) The mixed-derivative quantity: with $\alpha = \pi/4$ fixed and $\gamma_1 = \pi/2$, $\gamma_2 = \pi$,

$$D := \frac{\langle \partial_\alpha S \rangle_{\gamma_1} - \langle \partial_\alpha S \rangle_{\gamma_2}}{\gamma_2 - \gamma_1} = \frac{1}{\gamma_2 - \gamma_1} \int_{\gamma_1}^{\gamma_2} \frac{\partial^2 \ln Z}{\partial\alpha\, \partial\gamma}\, d\gamma, \qquad D_R := \frac{D}{\hat{D}},$$

where $\hat{D}$ is the tree-level value of $D$ at $\beta = 1$, so that $D_R = \beta$ at tree level; $0 < \hat{D} \leq 3$.

(iii) The normalised mixed derivative at a point: $M_R(\alpha, \gamma) := (\partial^2 \ln Z/\partial\alpha\, \partial\gamma)/M_{\rm cl}$, where $M_{\rm cl} = 3\cos((\gamma - \alpha)/L^2)$ is its tree-level value at $\beta = 1$ (from (1)); unless stated otherwise $M_R$ is taken at the symmetric point $(\pi/4, 3\pi/4)$.

(iv) $h := \beta_R - D_R$.

The equality in (ii) holds because $\partial_\alpha \ln Z = -\langle \partial_\alpha S \rangle$. In the Monte Carlo, $D$ is obtained from two independent runs, one at $\gamma_1$ and one at $\gamma_2$, measuring only $\partial_\alpha S$. This estimator has a statistical error two to six times smaller than the covariance estimator $\langle \partial_\alpha S\, \partial_\gamma S \rangle - \langle \partial_\alpha S \rangle \langle \partial_\gamma S \rangle$ of the same derivative.

**Lemma 2.2** (no contact term; one-sided terms drop out)**.** *$\partial^2 S/\partial\alpha\, \partial\gamma = 0$, so $\partial^2 \ln Z/\partial\alpha\, \partial\gamma = \langle \partial_\alpha S\, \partial_\gamma S \rangle - \langle \partial_\alpha S \rangle \langle \partial_\gamma S \rangle$. If $\Gamma = f_1(\alpha) + f_2(\gamma) + g(\alpha, \gamma)$ then $\partial_\alpha \partial_\gamma \Gamma = \partial_\alpha \partial_\gamma g$.*

*Proof.* The angle $\alpha$ enters $S$ only through the plaquettes touching the lower boundary, and $\gamma$ only through those touching the upper boundary. For $L \geq 2$ no plaquette touches both. The rest is differentiation under the integral sign (the integrand is smooth and the group compact) and the vanishing of $\partial_\alpha \partial_\gamma$ on functions of one variable. □

By contrast, $\beta_R$ contains $f_1'(\pi/4) - f_2'(3\pi/4)$. This is the whole reason for introducing $D_R$: $h$ measures, roughly, how much of $\beta_R$ is carried by one-boundary terms and by the non-trivial dependence of $g$ on $(\alpha, \gamma)$ beyond $\gamma - \alpha$.

# 3 One loop

## 3.1 What is cited and what is computed

At one loop $\Gamma = \beta s_0 + \Gamma_1 + O(1/\beta)$ with $s_0 = S_{\rm cl}/\beta$. With $\beta = \beta(\mu) - 8b_0 \ln(a\mu)$, $8b_0 = 11/(3\pi^2) = 0.37151$ for SU(2), finiteness of $\Gamma$ requires

$$\Gamma_1(\alpha, \gamma) = -8b_0 \ln(L/a)\, s_0(\gamma - \alpha) + F(\alpha, \gamma) + O(a/L).$$

That the logarithm multiplies $s_0$ and that no other logarithmic (boundary) counterterm appears is the renormalisability statement of [2]: the Seeley–DeWitt coefficient that produces the pole is a volume integral of $\mathrm{tr}\, G_{\mu\nu} G_{\mu\nu}$ and has no boundary term [2, (3.28), (3.36)]. It follows by hand that $\beta_R$ and $D_R$ have the same one-loop logarithm $-8b_0 \ln(L/a)$, i.e. the same one-loop step $8b_0 \ln 2 = 0.2575$ under $L \to 2L$, while the constants

$$\beta_R = \beta - 8b_0 \ln(L/a) + c_\eta + \ldots, \qquad D_R = \beta - 8b_0 \ln(L/a) + c_D + \ldots$$

may differ, because $F$ is not a function of $\gamma - \alpha$ alone. Indeed the background field strength depends only on $\gamma - \alpha$, but the constant part $\alpha/L$ of the spatial background is a holonomy $e^{2i\alpha}$ seen by the charged fluctuations, which cannot be gauged away.

We computed $\Gamma_1(\alpha, \gamma)$ directly on the lattice. The computation uses the second variation of the SU(2) Wilson action around the SF background, without any further approximation of the action; the ghost operator on $1 \le x^0 \le L-1$ together with the constant boundary mode of [2, (6.3)]; and $\Gamma_1 = \frac{1}{2} \ln\det(H + \lambda DD^\dagger) - \ln\det(D^\dagger D)$, decomposed into charge sectors and spatial momenta. Derivatives in $\alpha, \gamma$ are taken by a nine-point stencil with Richardson extrapolation. As a check, the one-loop coefficient $m_1(L) = -\beta_R^{(1)}/4$ of the SF coupling agrees with Table 1 of [2] to eight digits for $L/a = 6, 8, 10, 12, 16, 20, 24$ (for example 0.35422030, 0.45347745, 0.49316916). Further checks: gradient of the action at the background $3 \times 10^{-17}$; $|HD| \le 10^{-15}$ (the kernel of the Hessian is the gauge orbit); dependence on the gauge parameter $\lambda$ only through the constant $\frac{1}{2} n_g \ln\lambda$.

### 3.2 Results

Table 1 lists the one-loop coefficients (the part of each quantity proportional to $\beta^0$, in units where the tree level is $\beta$). Here $M_R^{(1)}$ is the mixed derivative at the symmetric point $(\pi/4, 3\pi/4)$, and $D_R^{(1)}$ is the average over $\gamma \in [\pi/2, \pi]$ used in the Monte Carlo.

Table 1: One-loop coefficients on the lattice, SU(2), Wilson action, $c_t = 1$.

| $L/a$ | $M_R^{(1)}$ | $D_R^{(1)}$ | $\beta_R^{(1)} = -4m_1$ | $\beta_R^{(1)} - D_R^{(1)}$ | neutral $M_R^{(1)}$ | charged $M_R^{(1)}$ |
|---|---|---|---|---|---|---|
| 4 | −0.93558 | −0.94624 | −1.25205 | −0.3058 | −0.2349 | −0.7007 |
| 6 | −1.17123 | −1.17290 | −1.41688 | −0.2440 | −0.2386 | −0.9326 |
| 8 | −1.30854 | −1.30779 | −1.53482 | −0.2270 | −0.2412 | −1.0673 |
| 10 | −1.40695 | −1.40524 | −1.62577 | −0.2205 | −0.2429 | −1.1640 |
| 12 | −1.48425 | −1.48205 | −1.69932 | −0.2173 | −0.2441 | −1.2402 |
| 16 | −1.60239 | −1.59973 | −1.81391 | −0.2142 | −0.2455 | −1.3568 |
| 20 | −1.69172 | −1.68885 | −1.90164 | −0.2128 | −0.2464 | −1.4453 |
| 24 | −1.76361 | −1.76064 | −1.97268 | −0.2120 | −0.2470 | −1.5166 |

We fit $b \ln N + c + d/N + e/N^2$ ($N = L/a \ge 8$):

- free $b$: $M_R^{(1)}$ gives $b = -0.37488$, which is 1.009 times $-8b_0$; $D_R^{(1)}$ gives $-0.37432$ (1.008 times); $\beta_R^{(1)}$ gives $-0.36979$ (0.995 times); the free $b$ of $M_R^{(1)}$ moves by 1–3% with the fit range;
- $b$ fixed at $-8b_0$: $c_M = -0.600(3)$, $c_D = -0.598(3)$, $c_\eta = -0.8099$, the last to be compared with $-4r_0 = -0.8094$ from [2, (7.39)]; the errors are the spread over fit ranges and forms, not statistical;
- the difference $\beta_R^{(1)} - M_R^{(1)}$ has a fitted logarithmic coefficient $+0.0051$, compatible with zero, and tends to $-0.21$.

The doubling steps of $M_R^{(1)}$ are 0.373, 0.294, 0.279 for $4 \to 8$, $8 \to 16$, $12 \to 24$, approaching 0.2575 from above. Those of $\beta_R^{(1)}$ are 0.283, 0.279, 0.273.

**Charged and neutral sectors.** The neutral sector contributes a constant ($M_R^{(1)} \to -0.247$) with no logarithm, and contributes nothing to the difference: the neutral part of $\beta_R^{(1)} - M_R^{(1)}$ is $+0.00186$, $+0.00012$, $+0.00001$, $0.00000$ at $L/a = 4, 8, 16, 24$, while the charged part is $-0.31833$, $-0.22639$, $-0.21153$, $-0.20907$. In the neutral sector $F$ is a function of $\gamma - \alpha$ only

(we checked $\partial_\alpha^2\Gamma_1 = -\partial_\alpha\partial_\gamma\Gamma_1$ there to $10^{-8}$), whereas the charged sector gives $(\partial_\alpha^2+\partial_\alpha\partial_\gamma)\Gamma_1 = -2.07$ at $L/a = 24$. U(1) has no charged fluctuations, so in this normalisation its one-loop $h$ is zero. This statement is a reading of the neutral-sector computation, not a separate U(1) computation.

**The edge $\gamma = \pi$.** The upper angle $\gamma = \pi$ lies on the edge of the fundamental domain of [2, (5.8)]: the upper holonomy is central and two charged zero modes appear, with lowest eigenvalue proportional to $\pi - \gamma$. Therefore $-\partial_\gamma^2\Gamma_1 \approx 1/(\pi-\gamma)^2$. We find 994, 995, 996 at $\gamma = 0.99\pi$ for $L/a = 4, 8, 16$, against $1/(0.01\pi)^2 = 1013$. The mixed derivative stays finite and smooth: $M_R^{(1)}(\pi/4, \gamma)$ varies by 2.5% over $\gamma \in [\pi/2, 0.99\pi]$ at $L/a = 16$. For $D_R^{(1)}$ the value at $\gamma_2 = \pi$ is a linear extrapolation from $\pi - 0.01$ and $\pi - 0.003$. Replacing $\gamma_2$ by $7\pi/8$ changes $D_R^{(1)}$ by less than 0.004 at $L/a = 24$.

**Summary of the weak-coupling end.** The quantities $D_R$ and $\beta_R$ have the same one-loop running. At one loop $h \to -0.21$, with the sign $D_R > \beta_R$. The difference $\beta_R - M_R$ at the symmetric point comes entirely from charged fluctuations.

# 4 Strong coupling

Let $u = I_2(\beta)/I_1(\beta)$ be the fundamental character coefficient of the SU(2) Wilson action ($u \approx \beta/4$ for small $\beta$). The spatial boundary plaquettes are trivial, so contractible surfaces do not depend on $\alpha, \gamma$; only surfaces bounded by loops winding around a spatial cycle at a boundary do. Two families give the lowest orders (counted by hand):

- one-sided strips (a winding loop at one boundary, closed by a U-shaped strip of area $3L$): $6L^2$ positions per boundary, each with weight $u^{3L}\chi(W)^2$, giving $\ln Z \supset B(\cos^2\alpha + \cos^2\gamma)$, $B = 24L^2u^{3L}$;
- cylinders joining the two boundaries (area $L^2$, and with one step, area $L^2 + L$): $\ln Z \supset A\cos\alpha\cos\gamma$, $A = 12L^2u^{L^2}(1 + 4(L-1)u^L)$.

The strips enter $\beta_R$ and, by Lemma 2.2, not $D_R$. With $s = \sin(\pi/(2L^2))$ their contribution is $\beta_R \supset -2B/(6L^2s) = -(8/s)u^{3L}$, and $8/s \geq 16L^2/\pi$. The cylinders contribute $A/(6L^2s)$ to $\beta_R$ and $A\sqrt{2}/(\pi\hat{D})$ to $D_R$. Their contribution to $h$ is therefore $(1/(6L^2s) - \sqrt{2}/(\pi\hat{D}))A$, and its coefficient is negative for $L \geq 4$. Both contributions have the same sign. Since $u^{L^2} \leq u^{3L}u^L$ for $L \geq 4$ and $0 \leq u \leq 1$, the cylinder term is of higher order than the strip term.

**Proposition 4.1** (conditional)**.** *Fix $L \geq 4$. Assume (H): the remainder $R$ of $h$ beyond the strip and cylinder terms satisfies $|R| \leq C_L u^{3L+1}$ for $0 < u \leq u_0$, with some $u_0 > 0$ and $C_L \geq 0$. Then, with $K = 8/s$ and $G = (1/(6L^2s) - \sqrt{2}/(\pi\hat{D}))A \leq 0$,*

$$h = -Ku^{3L} + G + R, \qquad |h - (-Ku^{3L} + G)| \leq C_L u \cdot u^{3L},$$

*and $h < 0$ for every $u \in (0, \min(u_0, u_1)]$, where $u_1 > 0$ is any number with $C_L u_1 < K$, i.e. for all $\beta$ below some $\beta_0(L) > 0$.*

*Structure of the proof.* The expansion of $\ln Z$ into the strip, cylinder and remainder terms and the coefficients $B$, $A$ are derived by hand. The remainder bound (H) is what one expects from the convergence of the polymer (cluster) expansion of Osterwalder and Seiler [4], but we have not derived it for this boundary geometry and use it as an assumption. Given these, the steps are: $3L + L \leq L^2$ for $L \geq 4$; $u^{L^2} \leq u^{3L}u^L$; $-2(24L^2u^n)/(6L^2s) = -(8/s)u^n$;

$8/s \geq 16L^2/\pi$ when $0 < s \leq \pi/(2L^2)$ (i.e. $\sin x \leq x$); $1/(6L^2 s) < \sqrt{2}/(\pi\hat{D})$ for $L \geq 4$, $0 < \hat{D} \leq 3$ and $s > x - x^3/4$ with $x = \pi/(2L^2)$; non-positivity of the cylinder part $G$, using $A \geq 0$; the bound on $|h - (-Ku^{3L} + G)|$ from (H) (in Lean stated for $-Ku^{3L} + R$, which is the same inequality since $G$ cancels); and $h < 0$ when $C_L u < K$, then on the whole interval $(0, \min(u_0, u_1)]$, by applying `h_neg_on_interval` with $u_0$ replaced by $\min(u_0, u_1)$. Each of these is a theorem of the Lean file described in §6 (Table 5), stated for abstract real numbers $K$, $C$, $G$, $R$. The inequalities $\sin x \leq x$ and $\sin x > x - x^3/4$, the bounds $\hat{D} \leq 3$ and $A \geq 0$, and (H) enter as hypotheses. □

We do not evaluate $C_L$ or $u_0$, and we do not claim a $\beta_0$ uniform in $L$ (the count of folded strips grows with $L$). For $L = 3$ one has $3L = L^2$ and for $L \leq 3$ the cylinder is leading, so this statement says nothing about the Monte Carlo points at $L/a = 3$, which in any case lie outside the range $L/a \geq 4$ required in [3, (2.9)]. Nor does it say anything about $\beta \geq 2$. At the measured points with $\beta \geq 2$ the leading strong-coupling term $(8/s)u^{3L}$ is between $3.6 \times 10^{-3}$ and $4.3 \times 10^{-2}$ for $L/a = 4$ and below $10^{-3}$ for $L/a = 6$ and 8. The negative values of $h$ at the largest $\bar{g}^2$ are about ten times this term (at $L/a = 4$, $\beta = 1.95$: $h = -0.027(6)$ against $(8/s)u^{12} \approx 2.8 \times 10^{-3}$) and are not explained by it.

# 5 Monte Carlo

## 5.1 Setup

We used heat-bath updates followed by overrelaxation sweeps (one overrelaxation per heat bath for $L/a \leq 4$, two for $L/a \geq 6$). Thermalisation was 200 sweeps (500 for $L/a = 3$, 300 for $L/a = 10$, whose runs do not appear in the tables of this note; 400 in the last U(1) series). We took one measurement per update cycle. For $D_R$ we used, from the second series on, the one-link integral at $x^0 = 1$: each term of $\partial_\alpha S$ is linear in one link at $x^0 = 1$, and the other factors of the term do not contain this link, so the link can be replaced by its conditional expectation without changing the expectation value. This reduces the variance by a factor 1.6 to 1.8. Plain and one-link estimates agree within errors at every point where both were taken. The quantity $\beta_R$ comes from separate runs at $(\pi/4, 3\pi/4)$. Errors are binned jackknife errors, taking the largest over bin widths $25, 50, 100, 200$. Errors of $\beta_R$ and $D_R$, which come from independent runs, are added in quadrature. Each run used one core of one laptop computer. The numbers of measurements per run are summarised in Table 2. Where several series exist at one point, the table of results uses their error-weighted mean.

Table 2: Monte Carlo series and measurements per run (one run per value of $\gamma$; $D_R$ needs two runs, $\beta_R$ one).

| Series | Points | Measurements per run |
|---|---|---|
| first | SU(2), U(1), $L/a \leq 8$ | 2000 (1500 at $L/a = 8$; one run 1250) |
| second | SU(2) $\beta = 1.6$–$2.5$, $L/a = 3$–$10$; U(1) | 6000–10000 |
| third | SU(2) $\beta = 1.6$–$2.3$, $L/a = 3$–$8$ | 5000–10000 |
| fourth | SU(2) near $h = 0$ and the maximum, $L/a = 4, 6, 8$ | 8000–96000 |
| fifth | U(1) $\beta = 0.8$–$1.3$, $L/a = 4, 6, 8$ | 16000–24000 |

## 5.2 SU(2)

Table 3 and Figure 1(a) give all 36 SU(2) points. For the points with $\beta_R \lesssim 0.04$ the relative error of $\beta_R$ is large and enters $\bar{g}^2 = 4/\beta_R$ directly. At three points ($L/a = 3$, $\beta = 1.6$; $L/a = 8$, $\beta = 2.28$ and 2.20) $\beta_R$ is compatible with zero, so their $\bar{g}^2$ is not determined (only bounded below).

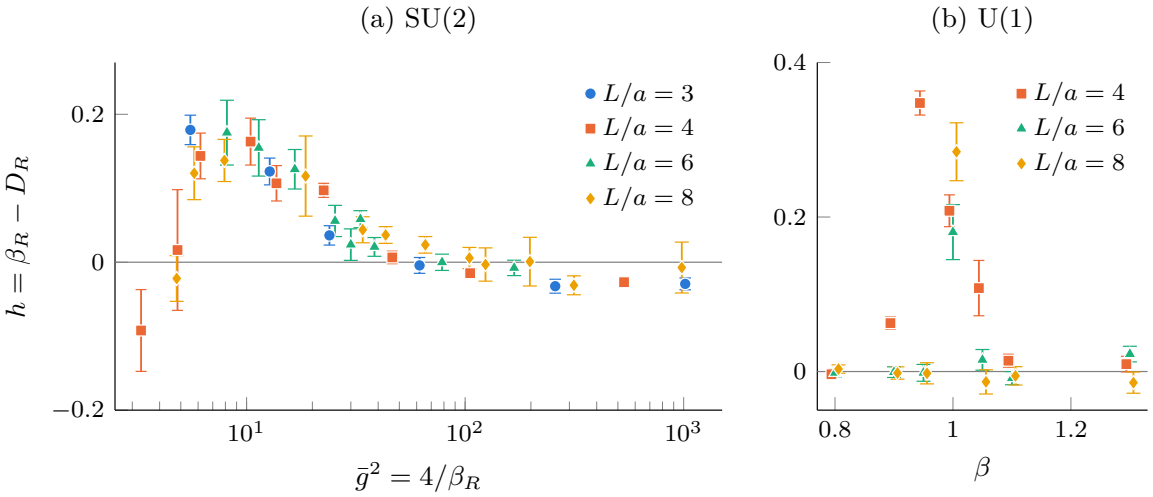


Figure 1: (a) SU(2): $h = \beta_R - D_R$ against $\bar{g}^2 = 4/\beta_R$ (logarithmic axis), by lattice size. (b) U(1): $h$ against $\beta$; the points of the three lattice sizes are shifted by $\pm 0.006$ in $\beta$ for legibility. Data: Tables 3 and 4.

**Shape.** Read from the table:

- near $\bar{g}^2 \approx 4.8$, $h$ is compatible with zero ($L/a = 4$: $+0.017(82)$ at 4.8; $L/a = 8$: $-0.022(31)$ at 4.8), and the only point below, $L/a = 4$ at $\bar{g}^2 = 3.3$, has $-0.092(55)$, on the side of the one-loop value $-0.21$;
- the maximum lies at $\bar{g}^2 \approx 5$ to 10 with height 0.14 to 0.18 ($L/a = 3$: 0.179(20) at 5.5; $L/a = 4$: 0.163(32) at 10.4; $L/a = 6$: 0.175(44) at 8.1; $L/a = 8$: 0.138(29) at 7.9); the differences between these four maxima are 0.1 to $1.2\sigma$;
- $h$ decreases to 0.02–0.10 for $\bar{g}^2 \approx 20$ to 40 and reaches zero for $\bar{g}^2 \approx 60$ to 120: by linear interpolation between neighbouring points in $\bar{g}^2$, 57.8 ($L/a = 3$), 64.4 ($L/a = 4$), 78.2 ($L/a = 6$, where one point is 0.000(11)) and 117 ($L/a = 8$);
- beyond $\bar{g}^2 \approx 150$, $h$ lies between $-0.03$ and 0.

For $L/a \geq 4$ and $\bar{g}^2 \approx 35$ to 140, points of different lattice sizes at comparable $\bar{g}^2$ agree within about $2\sigma$. The largest difference in this range is $2.1\sigma$, between $L/a = 8$ at $\bar{g}^2 = 43.3$ and $L/a = 4$ at 46.4. With comparable statistics at $L/a = 4$, 6 and 8, no systematic excess of $L/a = 8$ remains there. Outside this range the agreement is not uniform: $L/a = 3$ at $\bar{g}^2 = 23.9$ ($+0.036(13)$) and $L/a = 4$ at 22.5 ($+0.097(10)$) differ by $3.8\sigma$. The order $58 < 64 < 78 < 117$ of the zero crossings is suggestive of a drift with $L$, but no pair of points at the same $\bar{g}^2$ differs by $2\sigma$ in that region, and the $\bar{g}^2$ values there are poorly determined. We therefore regard the right-edge $L$-dependence as undecided.

Table 3: SU(2): $\beta_R$, $D_R$ and $h = \beta_R - D_R$ (combined series).

| $L/a$ | $\beta$ | $\bar{g}^2$ | $\beta_R$ | $D_R$ | $h$ |
|---|---|---|---|---|---|
| 3 | 2.20 | 5.53 | 0.7228(80) | 0.5439(182) | +0.179(20) |
| 3 | 2.00 | 12.8 | 0.3134(88) | 0.1907(158) | +0.123(18) |
| 3 | 1.90 | 23.9 | 0.1671(77) | 0.1308(107) | +0.036(13) |
| 3 | 1.80 | 61.9 | 0.0647(51) | 0.0690(94) | −0.004(11) |
| 3 | 1.70 | 258 | 0.0155(43) | 0.0479(84) | −0.032(9) |
| 3 | 1.60 | 1017 | 0.0039(44) | 0.0332(67) | −0.029(8) |
| 4 | 2.70 | 3.29 | 1.2142(123) | 1.3065(539) | −0.092(55) |
| 4 | 2.40 | 4.83 | 0.8276(196) | 0.8111(792) | +0.017(82) |
| 4 | 2.30 | 6.15 | 0.6505(104) | 0.5068(291) | +0.144(31) |
| 4 | 2.20 | 10.4 | 0.3834(230) | 0.2203(218) | +0.163(32) |
| 4 | 2.15 | 13.7 | 0.2920(116) | 0.1853(209) | +0.107(24) |
| 4 | 2.10 | 22.5 | 0.1775(54) | 0.0804(79) | +0.097(10) |
| 4 | 2.05 | 46.4 | 0.0862(46) | 0.0796(72) | +0.007(8) |
| 4 | 2.00 | 105 | 0.0379(36) | 0.0527(57) | −0.015(7) |
| 4 | 1.95 | 534 | 0.0075(32) | 0.0345(56) | −0.027(6) |
| 6 | 2.40 | 8.13 | 0.4923(224) | 0.3171(377) | +0.175(44) |
| 6 | 2.35 | 11.4 | 0.3519(170) | 0.1973(341) | +0.155(38) |
| 6 | 2.30 | 16.6 | 0.2407(139) | 0.1150(228) | +0.126(27) |
| 6 | 2.28 | 25.4 | 0.1575(109) | 0.1017(181) | +0.056(21) |
| 6 | 2.27 | 30.0 | 0.1334(106) | 0.1096(185) | +0.024(21) |
| 6 | 2.26 | 33.2 | 0.1205(58) | 0.0623(99) | +0.058(12) |
| 6 | 2.25 | 38.5 | 0.1040(64) | 0.0833(109) | +0.021(13) |
| 6 | 2.22 | 78.4 | 0.0510(58) | 0.0511(94) | −0.000(11) |
| 6 | 2.20 | 168 | 0.0239(52) | 0.0316(90) | −0.008(10) |
| 8 | 2.70 | 4.79 | 0.8355(127) | 0.8575(282) | −0.022(31) |
| 8 | 2.60 | 5.76 | 0.6944(148) | 0.5741(325) | +0.120(36) |
| 8 | 2.50 | 7.92 | 0.5052(121) | 0.3676(258) | +0.138(29) |
| 8 | 2.40 | 18.6 | 0.2147(391) | 0.0983(375) | +0.117(54) |
| 8 | 2.36 | 34.0 | 0.1176(92) | 0.0737(150) | +0.044(18) |
| 8 | 2.35 | 43.3 | 0.0924(53) | 0.0556(100) | +0.037(11) |
| 8 | 2.34 | 65.8 | 0.0608(52) | 0.0373(100) | +0.024(11) |
| 8 | 2.32 | 105 | 0.0382(66) | 0.0325(127) | +0.006(14) |
| 8 | 2.33 | 124 | 0.0323(112) | 0.0354(195) | −0.003(23) |
| 8 | 2.28 | 198 | 0.0202(153) | 0.0194(291) | +0.001(33) |
| 8 | 2.30 | 315 | 0.0127(62) | 0.0439(111) | −0.031(13) |
| 8 | 2.20 | 980 | 0.0041(252) | 0.0112(234) | −0.007(34) |

**Comparison with one loop in the renormalised coupling.** We take the measured $\beta_R$ as input, together with the lattice one-loop difference $\Delta(N) = D_R^{(1)} - \beta_R^{(1)}$ (Table 1). The prediction $D_R \approx \beta_R + \Delta(N)$ exceeds the measured $D_R$ at the five weak-coupling points of Table 3 ($\beta = 2.7$ and 2.4) by $\delta = 0.205(31)$ to $0.419(44)$. At the three points with $\bar{g}^2 \leq 4.83$, $\delta \cdot \beta_R$ is 0.259(67), 0.171(26) and 0.267(68), roughly 0.17 to 0.27 (weighted mean 0.19(2), $\chi^2 = 2.9$ for two degrees of freedom). A term $\delta \propto \bar{g}^2$ of this size is consistent with a next-order (two-loop) correction, but three points do not determine its coefficient. At $\bar{g}^2 = 8.1$ and 18.6, $\delta \cdot \beta_R$ is 0.206(24) and 0.074(18). (The errors of $\delta \cdot \beta_R$ treat $\delta$ and $\beta_R$ as independent, although $\delta$ contains $\beta_R$; they are therefore only indicative.) We did not compute two loops.

### 5.3 U(1)

Table 4: U(1): $\beta_R$, $D_R$ and $h$ (normalised as for SU(2), tree level = $\beta$).

| | $L/a = 4$ | | | $L/a = 6$ | | | $L/a = 8$ | | |
|---|---|---|---|---|---|---|---|---|---|
| $\beta$ | $\beta_R$ | $D_R$ | $h$ | $\beta_R$ | $D_R$ | $h$ | $\beta_R$ | $D_R$ | $h$ |
| 0.80 | 0.003 | 0.007 | −0.004(4) | −0.001 | 0.001 | −0.002(5) | −0.001 | −0.005 | +0.003(5) |
| 0.90 | 0.051 | −0.012 | +0.063(8) | −0.000 | 0.000 | −0.001(7) | −0.004 | −0.002 | −0.002(8) |
| 0.95 | 0.353 | 0.005 | +0.348(16) | 0.008 | 0.009 | −0.002(11) | 0.002 | 0.004 | −0.002(14) |
| 1.00 | 0.579 | 0.371 | +0.208(21) | 0.508 | 0.327 | +0.181(36) | 0.443 | 0.159 | +0.285(38) |
| 1.05 | 0.670 | 0.562 | +0.108(36) | 0.669 | 0.653 | +0.015(13) | 0.659 | 0.673 | −0.013(16) |
| 1.10 | 0.764 | 0.750 | +0.014(8) | 0.748 | 0.756 | −0.009(9) | 0.740 | 0.745 | −0.006(12) |
| 1.30 | 1.006 | 0.996 | +0.010(10) | 1.002 | 0.979 | +0.023(10) | 0.980 | 0.994 | −0.014(14) |

The data are in Table 4 and Figure 1(b). Deep in the Coulomb phase ($\beta = 1.1$, 1.3) and in the confined phase ($\beta = 0.8$, and 0.9, 0.95 for $L/a \geq 6$), $h$ is compatible with zero (largest deviation $2.2\sigma$). In the Coulomb phase $D_R$ is compatible with a constant in $L$ (for example 0.750(8), 0.756(8), 0.745(11) at $\beta = 1.1$), as expected from the free photon, while $\beta_R$ decreases slightly with $L$ (about −0.025 from $L/a = 4$ to 8, 4 to $5\sigma$). At the transition $h$ has a peak: at $L/a = 4$ it spans $\beta = 0.90$ to 1.05 (maximum 0.348(16) at 0.95, where $\beta_R$ has risen to 0.35 and $D_R$ is still zero); at $L/a = 6$ and 8 only the point $\beta = 1.00$ is non-zero, 0.181(36) and 0.285(38). The width shrinks below the $\beta$ spacing 0.05 of our scan, but the height at $\beta = 1.00$ does not decrease from $L/a = 6$ to 8. The $L/a = 6$ run at $\beta = 1.00$ had not settled (block averages drifting over the first three eighths), so its error may be underestimated.

**Separation.** Away from the transition, $|h| \leq 0.023$ at all U(1) points, while the SU(2) maxima 0.14 to 0.18 are 3.4 to $7\sigma$ above 0.023(10) (errors of both combined). At the transition the U(1) peak is as high as or higher than the SU(2) maximum, so the size of $h$ alone separates the two theories only away from the U(1) transition. The two theories are not compared at the same $\bar{g}^2$: the U(1) Coulomb points have $\bar{g}^2 = 1/\beta_R \approx 1.0$ to 1.35, and in the confined phase $\beta_R \approx 0$.

# 6 What is machine-checked

## 6.1 Inside and outside Lean

| Step | Status |
|---|---|
| Lemma 2.2 (no contact term) | by hand |
| one-loop renormalisability, logarithm $\propto s_0$ | cited [2] |
| one-loop numbers, Table 1 | floating-point computation |
| coefficients $A \geq 0$, $B$ of the strong-coupling terms | by hand |
| remainder bound (H) | assumption: it contains the convergence of the expansion (expected from [4], not derived) and the completeness of the hand count of the terms up to order $u^{3L}$ |
| $\sin x \leq x$, $\sin x > x - x^3/4$, $\hat{D} \leq 3$, $A \geq 0$ | hypotheses of the Lean theorems |
| arithmetic and inequalities of Proposition 4.1 | Lean (9 theorems) |
| Monte Carlo numbers, Tables 3, 4 | floating-point Monte Carlo |

## 6.2 The Lean file

The file `StrongCouplingOneSidedTerm.lean` (namespace `StrongCouplingOneSided`, 9 theorems, sha256 `1fd998eea20a83e74212a2ccd61c124d8ff125ffe0f9f6e1f58a2136db4bafb2`) is a single file beginning with `import Mathlib`. It is distributed as a self-contained bundle for this note (bundle: `https://computoergosum.com/principia/lean/principia-ym-boundary-mixed-derivative-2026-10-29.tar.gz` with checksum file `https://computoergosum.com/principia/lean/principia-ym-boundary-mixed-derivative-2026-10-29.tar.gz.sha256`; axiom log: `https://computoergosum.com/principia/lean/axioms-ym-boundary-mixed-derivative-2026-10-29.txt`; ledger of the site's Lean material: `https://computoergosum.com/en/principia/lean/index.html`). The file was checked with Lean v4.33.1 and Mathlib v4.33.1 (commit `0df444a3`); the bundle holds the file, a README and the axiom log, and is not a Lake project. To verify: extract the bundle, place the file in a Lean 4 project that depends on Mathlib at that version, run `lake exe cache get` there, then run `LEAN_NUM_THREADS=1 lake env lean StrongCouplingOneSidedTerm.lean`; the nine `#print axioms` lines at the end of the file must each print `[propext, Classical.choice, Quot.sound]`, as recorded in the axiom log. The file contains no `sorry`, no `axiom` declaration and no `native_decide`. The two key statements, verbatim:

- `theorem tube_coeff_neg (L s D : ℝ) (hL : 4 ≤ L)`
  `(hs : π/(2*L^2) - (π/(2*L^2))^3/4 < s) (hD0 : 0 < D) (hD : D ≤ 3) :`
  `1/(6*L^2*s) < √2/(π*D)`
- `theorem h_neg_on_interval (K C u u₀ R G : ℝ) (L : ℕ) (hu : 0 < u)`
  `(hu0 : u ≤ u₀) (hC : 0 ≤ C) (hR : |R| ≤ C*u^(3*L+1)) (hCu0 : C*u₀ < K)`
  `(hG : G ≤ 0) : -K*u^(3*L) + G + R < 0`

What the kernel checks is the arithmetic: that these inequalities follow from their hypotheses. That the hypotheses hold for the lattice gauge theory (the expansion, its coefficients and its convergence) is not checked by Lean. The Lean file covers only the arithmetic of §4. The one-loop and Monte Carlo results, which are the bulk of this note, are floating-point computations outside Lean.

# 7 What is not claimed

- **No rigorous control of the intermediate region.** For $\bar{g}^2$ between the weak-coupling end and the strong-coupling end there is no rigorous tool here. The shape of $h$ there is a Monte Carlo observation.
- **No separation by the doubling step.** The Monte Carlo separates the two theories only by the size of $h$, and only away from the U(1) transition; we do not show a separation by the change of a quantity under one doubling $L \to 2L$. Doubling steps appear only in the one-loop computation of §3.
- **Point-by-point agreement is limited.** Agreement within about $2\sigma$ between lattice sizes holds for $L/a \geq 4$ and $\bar{g}^2 \approx 35$ to 140. When $L/a = 3$ is included, the points near $\bar{g}^2 \approx 23$ differ by $3.8\sigma$.
- **The $L$-dependence at the right edge is undecided.** The zero crossings move from $\bar{g}^2 \approx 58$ to 117 as $L/a$ goes from 3 to 8, but point-by-point differences stay below $2\sigma$ there, and the $\bar{g}^2$ values are poorly determined. At three points $\beta_R$ is compatible with zero and $\bar{g}^2$ is not determined. Nor do we claim that the position or height of the maximum is independent of $L$; we only find no difference beyond $1.2\sigma$ between the maxima.
- **Limited precision at $L/a = 8$.** Near the maximum the $L/a = 8$ points are sparse ($\bar{g}^2 = 7.9$ and 18.6 have errors 0.029 and 0.054). No continuum extrapolation is attempted. The lattice size $L/a = 3$ is outside the range $L/a \geq 4$ required in [2, 3].
- **Not a comparison of U(1) and SU(2) at the same $\bar{g}^2$.** U(1) points have $\bar{g}^2 \approx 1$ or $\beta_R \approx 0$. The separation statement holds only away from the U(1) transition, and we do not claim that the U(1) peak disappears as $L \to \infty$.
- **Strong coupling.** Proposition 4.1 is conditional on (H), which is expected from [4] but not derived, and on the hand-derived coefficients. We do not give $C_L$, $u_0$ or a $\beta_0$ uniform in $L$, and we do not consider $c_t \neq 1$.
- **One loop.** There is no two-loop computation. The constants $c_M$, $c_D$ carry a fit-range error of about 0.003. The value of $D_R^{(1)}$ at $\gamma_2 = \pi$ is a one-sided extrapolation, and $\gamma = \pi$ exactly (with the zero modes treated as collective coordinates) was not computed. The comparison with Monte Carlo in the renormalised coupling rests on three points and does not determine a two-loop coefficient. That the one-loop $h$ vanishes for U(1) is a reading of the neutral-sector computation, not a separate U(1) computation.
- **Monte Carlo.** All runs were made on one laptop computer, one core per run, with 1250 to 96000 measurements per run (Table 2). Integrated autocorrelation times were not measured (errors are binned jackknife). The quantities $\beta_R$ and $D_R$ come from independent runs.
- This note does not address the mass gap, a continuum limit, or the existence of the theory.

# 8 Correspondence table

Table 5 lists the steps of Proposition 4.1 and the Lean declarations. All declarations are in the namespace `StrongCouplingOneSided` of the file `StrongCouplingOneSidedTerm.lean`. The Lean statements are about abstract real numbers $K$, $C$, $G$, $R$, $u$. The identification $K = 8/s$,

$G = (1/(6L^2 s) - \sqrt{2}/(\pi \hat{D}))A$ is made in §4. The row `h_main_term` is a restatement of the hypothesis (H), not a further step.

Table 5: Steps of Proposition 4.1 and the Lean declarations.

| Statement | Lean declaration | Line |
|---|---|---|
| $3L + L \le L^2$ for $L \ge 4$ | `four_mul_le_sq` | 17 |
| $u^{L^2} \le u^{3L} u^L$ for $0 \le u \le 1$ | `area_le_strip` | 21 |
| strip term $= -(8/s)u^{3L}$ | `strip_term_eq` | 27 |
| $8/s \ge 16L^2/\pi$ (given $0 < s \le \pi/(2L^2)$) | `strip_coeff_lower` | 33 |
| cylinder coefficient negative | `tube_coeff_neg` | 43 |
| $cA \le 0$ for $c < 0$, $A \ge 0$ | `tube_part_nonpos` | 70 |
| $\lvert R\rvert \le Cu^{3L+1} \Rightarrow \lvert(-Ku^{3L} + R) - (-Ku^{3L})\rvert \le Cu \cdot u^{3L}$ | `h_main_term` | 74 |
| $-Ku^{3L} + G + R < 0$ if $G \le 0$, $\lvert R\rvert \le Cu^{3L+1}$, $Cu < K$ | `h_neg` | 81 |
| the same for all $u \in (0, u_0]$ if $Cu_0 < K$, $C \ge 0$ | `h_neg_on_interval` | 91 |

# 9 Disclosure of AI use

Two of the three authors are AI agents. *Shiori* and *Rin* are instances of Claude (Anthropic), run as the coding agent Claude Code. The definitions, the one-loop and Monte Carlo programs and runs, the strong-coupling counting, the Lean 4 file including the formalised statements, and this text were produced by Shiori over many sessions, which share no memory and rely on the written record; further sessions of Shiori reviewed the text against the Lean statements. Rin re-checked the Lean development from the distributed archive, confirmed that the declarations cited here are in it, and prepared the web edition. Kiichi, the human author, set the task and the working rules and decides what is published; he is responsible for this note.

This note has not been refereed. All review was done by further instances of the same model family, which share the authors' blind spots. What the Lean kernel checks is checked; everything else is the authors' word. Here the Lean check covers only the arithmetic of §4; the one-loop and Monte Carlo results are floating-point computations outside Lean.

**Revision history.** Revised 2026-11-14: the title and abstract are narrowed to what the Monte Carlo data show (separation only away from the U(1) transition, not at equal coupling); the content of assumption (H) is stated in the abstract; the size of the strong-coupling term at $\beta \ge 2$ is corrected; several statements of the abstract are qualified; a reference to background material outside the note is removed, so that the note stands alone. Revised 2026-11-15: the text was rewritten for readability. In addition, the second item of §7 now states the separation as the abstract does (by the size of $h$ only, and only away from the U(1) transition), and the value of $\bar{g}^2$ in the first item of the description of the shape was corrected to 4.8; the statements, proofs, numbers and tables are otherwise unchanged. The description of how the Lean files are distributed and checked was corrected.

# References


[1] A. Jaffe, E. Witten, *Quantum Yang–Mills theory*, in: The Millennium Prize Problems, Clay Mathematics Institute, 2006, 129–152 (not consulted directly).

[2] M. Lüscher, R. Narayanan, P. Weisz, U. Wolff, *The Schrödinger functional — a renormalizable probe for non-abelian gauge theories*, Nucl. Phys. B384 (1992) 168–228, arXiv:hep-lat/9207009.

[3] M. Lüscher, R. Sommer, U. Wolff, P. Weisz, *Computation of the running coupling in the SU(2) Yang–Mills theory*, Nucl. Phys. B389 (1993) 247–264, arXiv:hep-lat/9207010.

[4] K. Osterwalder, E. Seiler, *Gauge field theories on a lattice*, Ann. Physics 110 (1978) 440–471 (not consulted directly).